Clays and Clay Minerals, Vol. 66, No. 2, 127–137, 2018.

TUNING THE PHOTOPHYSICAL PROPERTIES OF CYANINE DYES WITH CLAY MINERALS

PETER BOHÁČ[1,*] AND JURAJ BUJDÁK[1,2]

[1] Institute of Inorganic Chemistry, Slovak Academy of Sciences, Dúbravská cesta 9, SK-845 36, Bratislava, Slovakia
[2] Comenius University in Bratislava, Department of Physical and Theoretical Chemistry, Faculty of Natural Sciences, Ilkovičova 6, SK-841 04, Bratislava, Slovakia

Abstract—Dye molecular aggregation and other interactions on clay mineral surfaces cause phenomena such as methachromasy (change in color), fluorescence enhancement, or quenching, which represent significant changes in the spectral properties of the dye. These phenomena can be used to control the photophysical properties of hybrid systems based on cationic organic dyes. In the present study, the aggregation of two structurally similar cyanine dyes, 3,3'-diethyl-oxocyanine iodide (OxCy) and 3,3'-diethyl-2,2'-thiacyanine iodide (ThCy), in colloidal dispersions of three smectites (saponite, hectorite, and montmorillonite) was studied by absorption and fluorescence spectroscopy for a broad range of dye/smectite loadings. Spectral data were analysed by chemometric methods (principal component analysis, PCA, and multivariate curve resolution, MCR). Detailed analysis of the OxCy absorption spectra by the chemometric methods revealed the formation of two types of oblique aggregates exhibiting light absorption in both H- and J-bands. The existence of such similar aggregates, with similar splitting of excitation energies, appears to be related to the existence of two stable conformational isomers of this dye. On increasing the smectite CEC and dye/smectite loading, fluorescence quenching occurred. The ThCy dye exhibited a stronger tendency for molecular aggregation than OxCy. On increasing the smectite CEC, the formation of oblique aggregates with dominant H-bands also increased. On aging of the hybrid dispersions, equilibria of ThCy aggregates were shifted to the species with dominant J-bands. This behavior had a significant impact on the shape and intensity of the fluorescence emission of the hybrid dispersions. Using different smectites enables control of the dye aggregation and significant change to the photophysical properties of the hybrid systems. These systems can be used for the detailed study of the photophysical properties of cyanine dyes in various states. The colloidal systems with cyanine dyes can be used as precursors for the preparation of novel hybrid materials. In addition, the sensitive response of the photophysical properties of cyanine dyes to the clay mineral surface can be applied to the characterization of clay minerals.

Key Words—Absorption Spectroscopy, Chemometric Analysis, Cyanine Dye, Dye Aggregation, Fluorescence Spectroscopy, Smectite.

INTRODUCTION

Dye molecular aggregation in the colloidal systems with smectites is a well known phenomenon. Basic mechanisms for the interaction and the influence of smectite parameters on the photophysical properties of dyes have been proposed based on the findings of numerous studies that deal mainly with methylene blue and rhodamine dyes (Bergmann and O'Konski, 1963; Ogawa and Kuroda, 1995; Ogawa, 1998; Pomogailo, 2005; Bujdák, 2006). Two main types of molecular aggregates are characterized by their structure, arrangement of molecules, and spectral properties. H-aggregates (H means 'hypsochromic'), which are sandwich-type molecular assemblies, are characterized by a shift of the absorption band to higher energies with respect to monomers. J-aggregates are based on 'head-to-tail' assemblies in which association between molecules is either end-on, or with slight overlap. They exhibit a shift of the absorption bands to lower energies. The third type is oblique J-aggregates with split absorption band and with transitions to both higher and lower energies with respect to the monomers (Schulz-Ekloff *et al.*, 2002; Bujdák, 2006; Schoonheydt and Johnston, 2013). The coexistence of several species can contribute to complex spectral changes. The relationship between the spectral properties and the structure of molecular aggregates is explained by the molecular exciton theory, which interprets the changes in spectral properties using a model of exciton electrostatic coupling (López Arbeloa *et al.*, 1989, 2007). Significant spectral changes take place only with very strong electrostatic interactions that occur for the association of planar molecules, whereby small distances between interacting transition dipoles of neighboring molecules can be achieved (Roden *et al.*, 2008). The exciton coupling leads to a splitting of the excitation energy state of the monomers (E_M) into two levels, with lower (E_1) and higher energy (E_2). The energy difference (ΔE) between these new states can be modeled by equation 1 (Eisfeld and Briggs, 2006; López Arbeloa *et al.*, 2007):

* E-mail address of corresponding author:
peter.bohac@savba.sk
DOI: 10.1346/CCMN.2018.064090

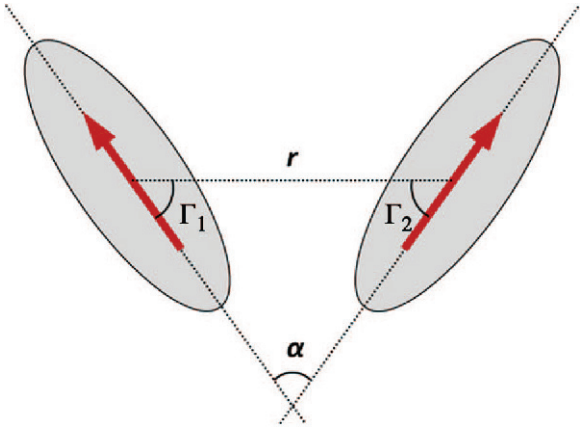

Figure 1. Schematic diagram explaining the parameters α, Γ_1, Γ_2, and *r* which characterize the arrangement of chromophoric units in a molecular dimer. The arrows show the orientation of the transition moments of the chromophores (López Arbeloa *et al.*, 2007).

$$\Delta E = \frac{2|M|^2(\cos\alpha + 3\cos\Gamma_1\cos\Gamma_2)}{r^3} \quad (1)$$

where *M* represents the transition dipole moment of the dye molecules in the monomeric state, α, Γ_1, and Γ_2 represent angles characterizing the structure of the aggregate (Figure 1).

The initial stage of dye adsorption and aggregation on the surface of smectites is a very fast process, limited by diffusion of the molecules, and its kinetics cannot be measured by conventional analytical methods (Gemeay *et al.*, 2002). Aggregates were probably formed initially prior to reaching the particle surface in the zones of electrical double layers that surround particles. Long reaction times are required to achieve spectral equilibrium (Pasternack *et al.*, 2000; Chibisov *et al.*, 2006; Baranyaiová and Bujdák, 2015). The slow changes in the spectra over time are related to the migration of the aggregates formed initially from the zones of diffuse electrical double layers toward the particle surface. The spectral changes observed in dye adsorption depend on the layer charge of the smectite particles (Bujdák *et al.*, 1998, 2002b; Baranyaiová and Bujdák, 2015). The effects of charge and other characteristics of colloidal particles have been studied extensively (Bujdák and Komadel, 1997; Bujdák *et al.*, 2001; Anedda *et al.*, 2005; Kaufhold, 2006). In addition to the effect of colloidal particles, the type of aggregates depends heavily on the specific dye properties. For example, methylene blue initially forms H-aggregates in smectite colloids, but these change over time to J-aggregates and monomers (Bujdák *et al.*, 2001). The opposite trend has been observed for rhodamine dyes, however (Lofaj and Valent, 2013; Baranyaiová and Bujdák, 2015).

Cyanine dyes are a type of organic dye which are able to form highly active J-aggregates in solutions, at interfaces, or in systems with colloids, polymers, or nanoparticles (Zhu, 1995; Kometani *et al.*, 2000; Tillmann and Samha, 2004; Yonezawa *et al.*, 2005; Behera *et al.*, 2007; Shapiro, 2007; Tani *et al.*, 2008; Würthner *et al.*, 2011; Hranisavljevic and Wiederrecht, 2012; Sato *et al.*, 2015; Shapiro *et al.*, 2016; Smirnov *et al.*, 2016). Except for pseudo-isocynanine (Ogawa *et al.*, 1996; Ono *et al.*, 1999; Miyamoto *et al.*, 2000; Bujdák *et al.*, 2003; Matejdes *et al.*, 2017a, 2017b; Valandro *et al.*, 2017), which is the most studied of the group, knowledge of the aggregation properties of other cyanine dyes in smectite systems is noticeably lacking. The adsorption of cyanine dyes on smectite particles can lead to significant changes in the photophysical and functional properties. In addition to molecular aggregation, other phenomena such as isomerization, conformational changes, photophysical phenomena, exciton coupling, redox processes, *etc.*, can influence the optical properties of the dye (Bujdák *et al.*, 2002a; Nakato *et al.*, 2014; Boháč *et al.*, 2016). Due to the variability of their properties, hybrid systems based on cyanine dyes are very interesting for both basic and applied research.

The objective of the present study was to find ways to tune the optical properties of colloidal systems, the components of which consisted of combinations of two cyanine dyes of similar structures and three smectites and which represented systems with (relatively) low, medium, and high layer charge. The principal relationships between the spectral properties and the selection of smectites and dye/smectite loading were investigated. The variation in component properties and dye/smectite loadings provides sufficient data to generalize some of the trends in the optical properties of such systems and provide guidance for the fabrication of functional hybrid materials.

MATERIALS AND METHODS

Synthetic Na^+-saponite Sumecton (Sap) and natural Na^+-montmorillonite (Mnt), purchased from Kunimine

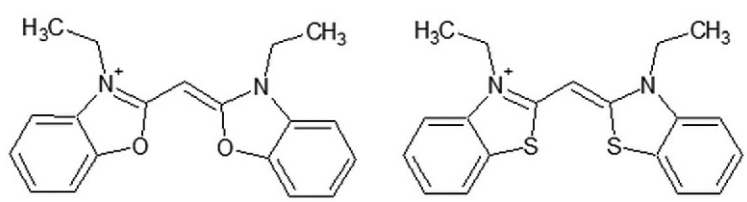

Figure 2. Molecular structure of the cationic cyanine dyes, OxCy (left) and ThCy (right).

https://doi.org/10.1346/CCMN.2018.064090 Published online by Cambridge University Press

Industries Co., Tokyo, Japan, and natural hectorite (Hec) from the Source Clays Respository of The Clay Minerals Society were used as host materials. Sap and Mnt were used without further purification. To improve the colloidal properties of natural Hec, the Na^+-form of Hec was prepared by an ion-exchange process (Bujdák *et al.*, 2002b). The cation exchange capacities of the smectites (CEC) were determined to be 0.87±0.05 (Sap), 1.08±0.04 (Hec), and 1.24±0.01 (Mnt) mmol/g by the Trien method (Czímerová *et al.*, 2006).

Two cationic cyanine dyes, 3,3′-diethyl-oxocyanine iodide (OxCy) and 3,3′-diethyl-2,2′-thiacyanine iodide (ThCy), were purchased from Sigma Aldrich, St. Louis, Missouri, USA, and used as received. The molecular structures of the dye cations are depicted in Figure 2. The basic properties of the dyes are listed in Table 1.

Sample preparation

Colloidal dispersions of layered silicates at concentrations of 1 g/L and 0.2 g/L were prepared using Millipore deionized water and stirred for 24 h at room temperature before use. Dye stock solutions with a concentration of ~1×10^{-4} mol/L were prepared using Millipore deionized water and stirred in the dark at room temperature for 1 h. The absorbance of the stock solution was then measured to determine the concentration of the dye, and new solutions with concentrations of 1×10^{-4} mol/L were prepared. Layered silicate dispersions were mixed with the dye solutions and the final dye concentration in the dye/smectite hybrid dispersions was always 5×10^{-6} mol/L. Systems were prepared with final dye/smectite ratios $n_{dye}/m_{smecite}$ of 0.01, 0.05, 0.1, 0.25, and 0.5 mmol/g, where n_{dye} and $m_{smecite}$ represent the amount of dye (mmol) and the mass of smectite (g), respectively. (The various ratios were achieved by varying the smectite concentrations.) For comparison, dye solutions of the same concentrations but without smectites were also prepared.

The samples of hybrid colloidal dispersions are labeled using the format dye/smecite/{n_{dye} /$m_{smecite}$/ loading}, *e.g.* OxCy/Sap/0.01 represents a hybrid system of OxCy and Sap with a dye/smectite loading of 0.01 mmol/g (the lowest loading prepared in the present experiments).

Experimental procedures

The absorption spectra of the colloidal suspensions were measured using a CARY 5000 spectrophotometer (Agilent, Santa Clara, California, USA). The absorption spectra were recorded 1 min after mixing the dye solution with the smectite colloidal dispersion at room temperature. The colloidal dispersions reached spectral equilibrium after 24 h. The absorption spectra of the dye/smectite hybrid systems were compensated by subtracting the baselines of the smectite colloidal dispersions from the raw spectra of the samples.

The emission spectra were measured using a fluorescence spectrophotometer FluoroLog 3 (Horiba Jobin Yvon, Kyoto, Japan). The measurements were performed at different excitation wavelengths for each dye independently (Table 1).

All measurements were carried out at room temperature.

Chemometric methods

Chemometric methods, principal component analysis (PCA), and multivariate curve resolution (MCR) were used to analyze the structure of the absorption spectra (using the software *Unscrambler*, Camo, Norway). Before the calculations, baseline subtraction was performed for all data, using non-linear fit with the function:

$$f_{bas}(\lambda) = \sum_{n=1-3} a_n \lambda^{-n} \quad (2)$$

where $f_{bas}(\lambda)$ and a_n represent the calculated parameters for each baseline. The calculations were carried out for the scattered light at selected ranges of wavelength for which no light absorption by dye molecules was observed. The correlation coefficients of the fits had values of >0.999. The effect of baseline subtraction was greatest for the samples with Mnt and those of high dye/smectite loadings. After subtracting the baselines, the spectra were arranged in matrices (one matrix for each dye) ready for chemometric calculations. The PCA method was applied to estimate the number of significant components. The method was set to perform calculations using mean-centered data, the SVD (singular value decomposition) algorithm, and full cross-validation. The MCR method is based on the alternating least squares algorithm (ALS) and constraints for the

Table 1. Spectral properties of the cationic cyanine dyes OxCy and ThCy.

Dye	M* (g/mol)	ε* (L/mol/cm)	$\lambda_{max\ A}$ (nm)	$\lambda_{max\ F}$ (nm)	λ_{excit} (nm)
OxCy	434.3	75 000 375	360	405	360
ThCy	466.4	81 300	422	472	400

* value obtained from the manufacturer

https://doi.org/10.1346/CCMN.2018.064090 Published online by Cambridge University Press

non-negativity of both the spectra and the concentrations were applied. Because of the bilinearity defined by the Beer-Lambert law, the matrices ($D_{sample\lambda}$) were decomposed to spectral (S_λ^T) and concentration matrices (C_{sample}).

$$D_{sample\ \lambda} = C_{sample} S_\lambda^T + E \quad (3)$$

E represents the matrix of residuals. The number of components was estimated from the result of the PCA method. With the MCR methods only a qualitative estimation of the spectra could be achieved. The proportion of the individual components in the samples was estimated from the concentration matrix and evaluated for dependence on the dye/smectite ratio and the type of smectite. The accuracy of the MCR calculations was estimated by the relevance of the spectral profiles and variable residuals. Due to the overlap of the spectra, the method could not estimate the spectral and concentration profiles reliably if the number of components was greater than three.

RESULTS AND DISCUSSION

The main spectral properties of aqueous solutions of cyanine dyes are shown by the normalized absorption and fluorescence spectra (Figure 3). The energy of the absorbed and emitted light decreased on substitution of the oxygen atom present in OxCy with the sulfur atom present in the ThCy cation. The absorption spectrum of OxCy consisted of two bands, the maxima of which were 1111 cm^{-1} apart. The spectrum of this dye persisted in almost the same form for the solutions in various solvents (not shown) and even in the colloidal dispersions with Sap (Figure 4a). For this reason, the existence of the second, less intense band was assigned not to molecular aggregation of the dye, but rather to the presence of two stable conformational isomers of the OxCy cation.

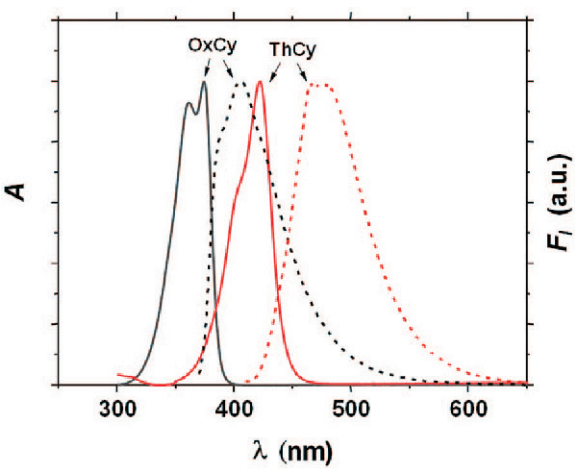

Figure 3. Normalized absorption (solid lines) and fluorescence spectra (dashed lines) of aqueous solutions of OxCy and ThCy. The excitation wavelengths were 360 nm (OxCy) and 400 nm (ThCy).

Spectral properties of 3,3′-diethyl-oxocyanine in smectite colloidal dispersions

The absorption spectra of OxCy in Sap colloidal dispersions did not depend significantly on the OxCy/Sap loading (Figure 4a). The spectra are composed of two absorption bands, similar to those of the dye in aqueous solution (Figure 3). The spectra did not change

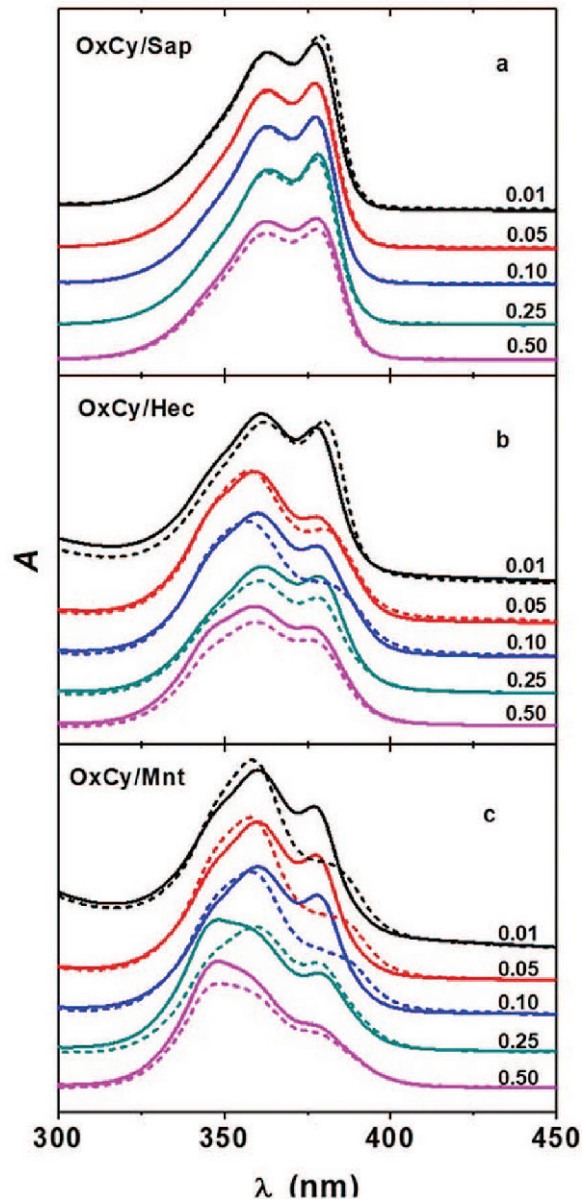

Figure 4. Absorption spectra of OxCy in smectite colloidal dispersions. Solid lines represent absorption spectra recorded immediately (~1 min) after mixing a dye solution and smectite colloidal dispersion, and dashed lines represent spectra recorded 24 h after mixing.

https://doi.org/10.1346/CCMN.2018.064090 Published online by Cambridge University Press

significantly with time. After 24 h (Figure 4a, dashed line), the most significant change was observed for the sample with the highest OxCy/Sap loading, 0.5 mmol/g. The reduction of absorbance over the entire spectral range in this case can be assigned to the partial destabilization of Sap colloids induced by neutralization of the negative charge of Sap particles by adsorption of OxCy dye cations. This destabilization of the colloids would lead to micro-flocculation of the particles and their settling with time. Changes of light scattering could also contribute to the overall spectral change. More significant spectral changes were observed in Hec colloidal dispersions (Figure 4b). A broadening of the main band and the appearance of a shoulder at lower wavelengths was the main feature of OxCy spectra observed for Hec colloids. The system least influenced was that with the lowest OxCy/Hec loading, 0.01 mmol/g. Hec is a natural smectite with a greater layer charge than Sap. The presence of Hec particles probably induced partial molecular aggregation of adsorbed OxCy cations, leading to spectral broadening and increased light absorption at lower wavelengths. The OxCy/Hec colloids also displayed more significant changes over time than the spectrally stable systems based on Sap. The spectral changes with time depended on the OxCy/Hec loading. A shift to longer wavelengths upon aging was observed for the lowest loading, 0.01 mmol/g. For the colloids of medium loadings, 0.02−0.25 mmol/g, a decrease in absorbance over time was mainly observed at longer wavelengths. The aggregates absorbing at shorter wavelengths were more stable. The sample with the greatest OxCy/Hec loading (0.5 mmol/g) exhibited a decrease in absorbance values over the whole spectral range. The most significant changes were observed for OxCy/Mnt colloids (Figure 4c). Even at the lowest loading, a significant quantity of dye aggregates was formed, but the species formed initially were unstable and changed over time.

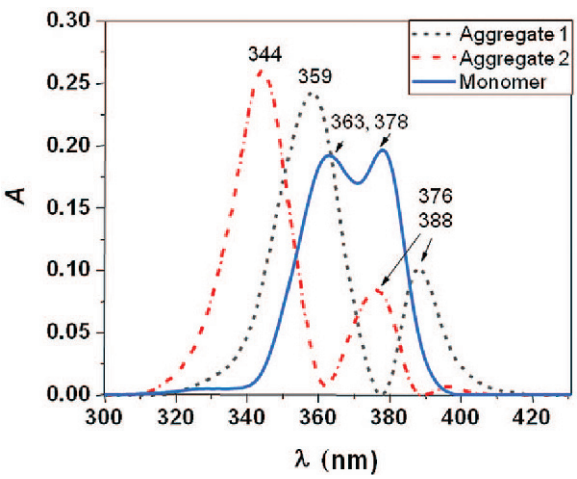

Figure 5. Spectral components of OxCy identified by the MCR analysis.

Dye molecular aggregates were mostly dominant in the samples with the greatest loadings, 0.25 and 0.50 mmol/g. In summary, OxCy is a chromophore with a relatively low tendency to form molecular aggregates when loaded on Sap which is the smectite sample with the lowest layer charge. However, in the colloids of the other two smectites, Hec and Mnt, which are characterized by a greater layer charge, dye molecular aggregates were detected clearly. The dye molecular aggregation also increased with the OxCy/smectite loading.

To better understand the spectral changes of OxCy in hybrid systems with smectites, the absorption spectra were analyzed by MCR and PCA methods. The MCR was able to identify three significant spectral components of OxCy (Figure 5) which could be used to reconstruct all spectra of OxCy/smectite colloidal dispersions with relatively small samples and variable residuals. The PCA confirmed this, with 96.1% of the variance explained by three components. The statistics could be improved significantly by going to four components (98.3%), but a strong overlap occurs between the spectra, so the calculation could lead to erroneous results. The spectral profiles showed very interesting results. The samples contained monomers and two oblique aggregates, both of which had both the H- and J-bands (Figure 5). The spectral profile of the monomers remains similar to that of the dye solution (Figure 3), which was most apparent in the spectra of OxCy in Sap colloids. The two types of aggregates seem to be related to one of the two isomers. For example, monomers that absorb at higher wavelengths (378 nm) form aggregates in which the excitation energy is split, resulting in two bands with maxima at 359 and 388 nm. A similar relation can be suggested between the monomers with a maximum at 363 nm and the aggregates absorbing at 344 and 376 nm. The greater intensity of the H-band than of the J-band indicates a relatively small angle, α, between the transition dipole moments of the molecules forming an aggregate (Figure 1). Using the ratio of the integral intensities of the two bands ($A_{\text{J-band}}$, $A_{\text{H-band}}$) and equation 4, the values of α were calculated. The values of these angles are very similar for both the components: ~53º and 51º for aggregates 1 and 2, respectively (Carbonaro, 2011).

$$\tan^2\left(\frac{\alpha}{2}\right) = \frac{A_{\text{J-band}}}{A_{\text{H-band}}} \quad (4)$$

Another feature is a similar energy splitting, at ~2470 and 2080 cm^{-1}, respectively (Figure 6). The greater splitting for the aggregates absorbing at higher energies could be due to shorter distances between interacting transition dipoles. The degree of splitting presumably reflects the structural features of the aggregate and how the molecules are packed together in it.

The concentrations of the components determined by the MCR analysis (Figure 7) support the interpretations

https://doi.org/10.1346/CCMN.2018.064090 Published online by Cambridge University Press

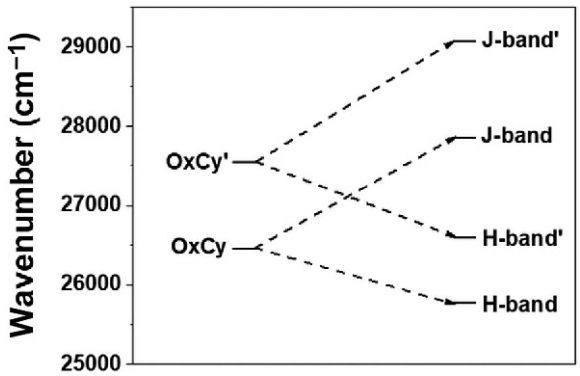

Figure 6. Energy splittings of the aggregates related to the two-dye isomers of OxCy.

obtained directly from the spectral data. Aggregation takes place more strongly in the systems based on Hec or Mnt. One of the aggregate types is formed preferentially in the Sap colloids, with no preference observed in Hec or Mnt colloids. As the total aggregation increased (Figure 7), the concentration of aggregate 1 increased, replacing monomers. The changes in the concentration of aggregate 2 were relatively small. The effect of loading seemed to be less significant than the surface properties of the smectite. After 24 h, the total amount of aggregates increased with loading, from ~19 to 27% for Sap, from ~32 to 51% for Hec, and from ~70 to 77% for Mnt samples. This is only an estimate as the MCR method does not detect differences in the extinction of the different spectral forms. The spectra of the components are normalized to a unit vector, which may affect the absolute values of the component concentrations, and only a rough quantitative estimate between the component concentrations is possible.

The variability of OxCy aggregation was also reflected in the large variability of the emission spectra (Figure 8). Whereas the absorption spectra of OxCy/Sap colloidal dispersions did not differ significantly from the spectrum of the OxCy solution (Figures 3, 4a), the fluorescence spectra for this series of samples changed significantly. Interestingly, OxCy/Sap colloids exhibited greater fluorescence than an aqueous solution of the same concentration (Figure 3). A similar phenomenon has been observed for ThCy dye (Boháč *et al.*, 2016). The enhanced fluorescence of cyanine dyes in saponite colloids can be attributed to the stabilization of dye conformers on the smectite surface. The dye adsorption and the electrostatic interaction on the surface of Sap particles prevent non-radiant rotational relaxation from their excited state, resulting in higher fluorescence yields. OxCy/Sap colloids of the lowest loadings

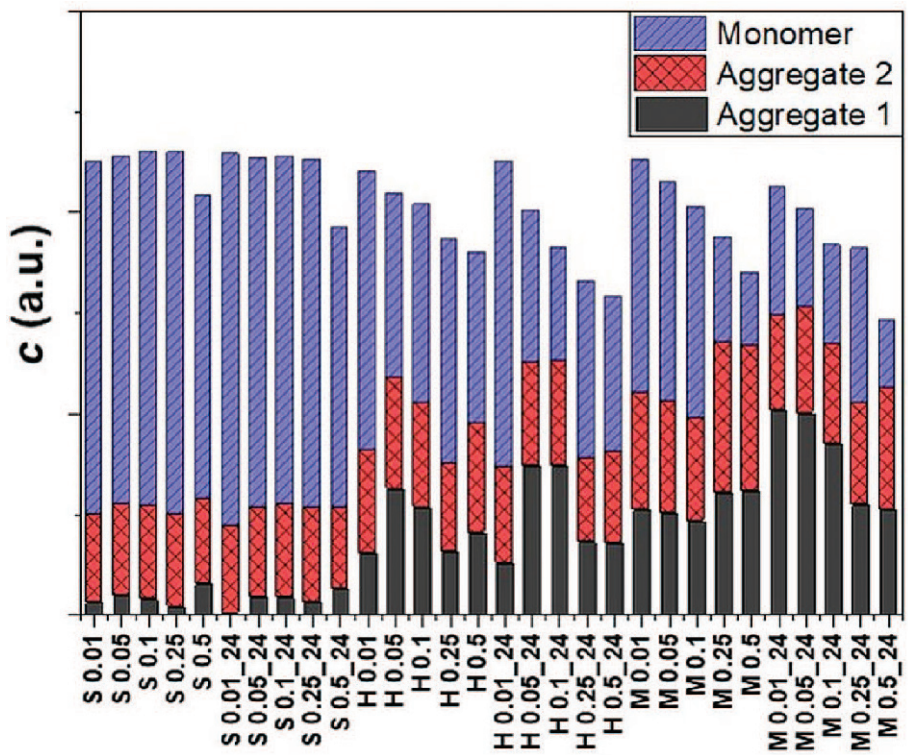

Figure 7. Concentrations of the spectral components of OxCy/smectite, as determined by MCR analysis. Markings on the horizontal axis indicate the identity of the samples. The abbreviations used indicate the smectite and the loading (mmol/g). The number '24' indicates that the spectra were measured after 24 h. The abbreviations of the clay-mineral names are as follows: S (saponite), H (hectorite), and M (montmorillonite).

https://doi.org/10.1346/CCMN.2018.064090 Published online by Cambridge University Press

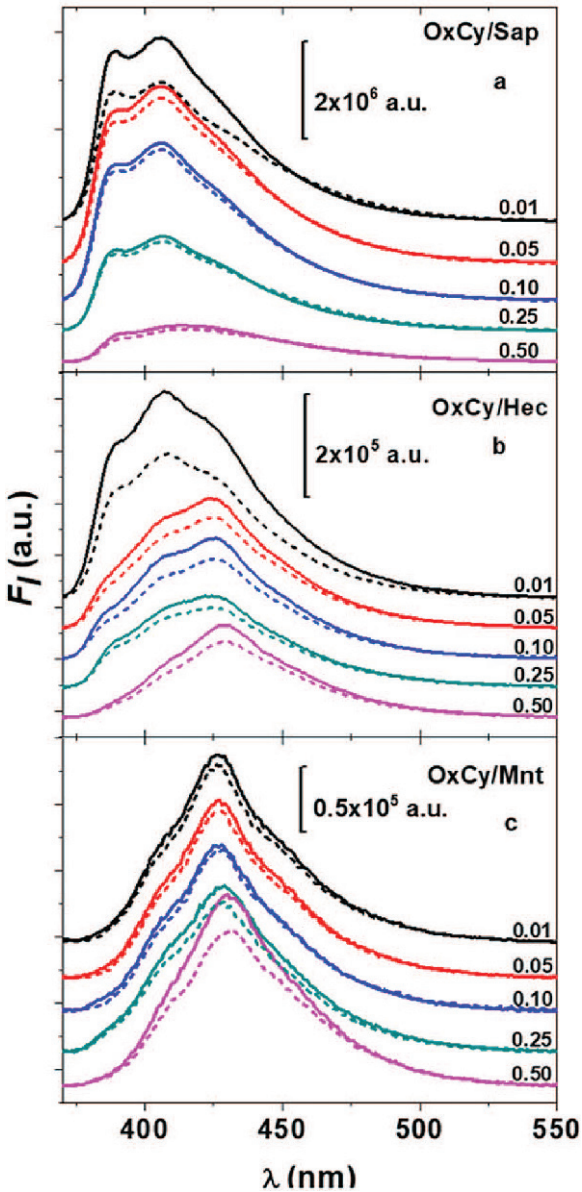

Figure 8. Emission spectra of OxCy in smectite colloidal dispersions. Solid lines represent absorption spectra recorded immediately (~1 min) after mixing the dye solution and smectite colloidal dispersion, and dashed lines represent spectra recorded 24 h after mixing.

(0.01−0.1 mmol/g) exhibited the greatest fluorescence of all tested samples containing this dye. At the highest loadings, 0.25 and 0.50 mmol/g, the fluorescence dropped significantly. Traces of very efficient fluorescence quenchers, most likely H-dimers or larger molecular aggregates, possibly were formed in some of OxCy/Sap colloids, and, while not visible in the absorption spectra (Figure 4a) due to their small amounts, could be identified by the MCR method (Figure 7). The high quenching efficiency was enhanced by excitation energy migration, which increased with the dye concentration; this may be expected to occur most at high loadings. Under these conditions, the excited OxCy molecules can be quenched efficiently by H-aggregates at relatively long distances. The process of energy migration that ends with energy transfer to the dye aggregates may be detected by way of a specific emission from the aggregate. However, the fluorescence quantum yields of molecular aggregates are generally very low and their signal could have been overwhelmed by emission from the monomers. For this reason the shape of the fluorescence spectra of OxCy/Sap colloids did not change significantly with increasing loading, nor was there any indication of the presence of another luminescent species. Colloids with Hec had significantly lower fluorescence than Sap colloids. The largest relative emission was observed for the OxCy/Hec colloid at the lowest loading, 0.01 mmol/g, which can be attributed to having the smallest amount of dye molecular aggregates, and hence the least fluorescence quenching. Even under these optimal conditions, however, the fluorescence of the OxCy/Hec colloids is always less than that of the OxCy/Sap colloid with the largest loading (0.50 mmol/g). The shape of the spectrum of OxCy/Hec at the lowest loading is somewhat similar to that of the OxCy/Sap colloids, emitting at relatively low wavelengths. On the other hand, OxCy/Hec colloids with greater dye loadings emit at relatively high wavelengths. Their spectra probably represent a weaker emission by molecular aggregates, for which additional evidence is provided by the spectra recorded for OxCy/Mnt colloids, which feature a single emission band positioned at longer wavelengths, and the spectra of which do not change with OxCy/Mnt loading. The intensity of emitted light recorded for OxCy/Mnt was, furthermore, reduced significantly compared to the values for OxCy/Hec colloids. With aging of the dispersions, a decrease in the intensities of the fluorescence spectra was observed which can be assigned to the partial destabilization of the colloids, resulting in microflocculation of the particles and their settling with time.

Spectral properties of 3,3′-diethyl-2,2′-thiacyanine in smectite colloidal dispersions

The large variations in the absorption spectra of ThCy clearly show the greater tendency of this dye toward molecular aggregation (Figure 9). The presence of sulfur atoms in the ThCy cation makes this compound more hydrophobic than OxCy and, therefore, more likely to aggregate. Relatively small changes were observed between ThCy/Sap colloid samples of different loadings. The main effect of loading for these systems is enhanced absorption at lower wavelengths in the sample of highest loading, 0.5 mmol/g. The formation of J-aggregates upon aging was indicated by spectral tailing to lower energies, especially for the samples with low ThCy/Sap loadings. Much larger changes were observed for the ThCy/Hec colloids. H-aggregates that absorb at lower

https://doi.org/10.1346/CCMN.2018.064090 Published online by Cambridge University Press

wavelengths were formed in fresh colloids at high loadings. Aging of the colloids, especially at low and medium loadings, resulted in a significant enhancement of absorbance at higher wavelengths, indicating the formation of J-type assemblies replacing H-aggregates over time. The colloids based on Mnt exhibited very similar trends to those of Hec colloids. The tendency toward H-aggregate formation was somewhat greater, as observed for the samples of higher dye loading.

The MCR analysis identified three components which, together, were able to explain 97% of the variances in the ThCy/smectite samples (Figure 10). One of the components represents monomers, the spectral profile of which is similar to that of the ThCy solution (Figure 3). Two types of aggregates were identified.

One type was H-aggregates of non-ideal sandwich-type structure with a dominant H-band at 398 nm and a smaller J-band at 437 nm. The ratio between these indicates that the angle between the transition moments of the molecules in the aggregate is ~50º.

The other type was J-aggregates with a broad J-band around 450 nm and a doublet of smaller H-bands in the range 380–420 nm. The complex character of this spectrum indicates variation in the spectral properties of the J-aggregates and possibly coexistence of J-aggregates of different structure or size.

The results are similar to those obtained by the recently published chemometric analysis of similar systems (Boháč *et al.*, 2016). Similar to OxCy (Figure 7), the aggregation of ThCy is more significant in the systems based on Hec or Mnt (Figure 11). More aggregation of ThCy than of OxCy was also observed for Sap systems, however. In general, the smaller amounts of monomers, especially at the highest loadings, could be due not only to the molecular aggregation, but also to the flocculation of colloidal dispersions. The effect of the loading was significantly less than that of the surface properties of smectites. The total amount of aggregates in the samples measured after 24 h increased with dye loading, ranging from ~34 to 41% for Sap, from ~52 to 60% for Hec, and from ~60 to 61% for Mnt colloids. J-aggregates were formed in relatively large amounts on aging, becoming prevalent in aged Hec and Mnt colloids. In the latter, the amount of J-aggregates increased on aging from an average of 10.5% to 46%. One might assume that H-aggregates formed upon mixing in the zones of electrical double layers surrounding the particles, and were converted to J-aggregates over

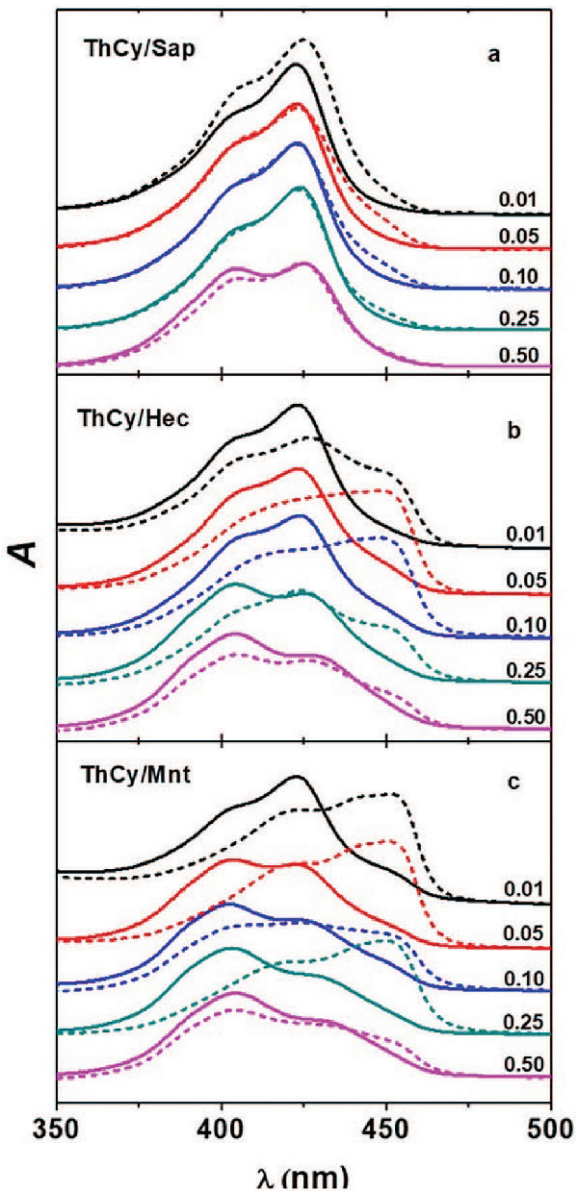

Figure 9. Absorption spectra of ThCy in smectite colloidal dispersions. Solid lines represent absorption spectra recorded immediately (~1 min) after mixing the dye solution and smectite colloidal dispersion, and dashed lines represent spectra recorded 24 h after mixing.

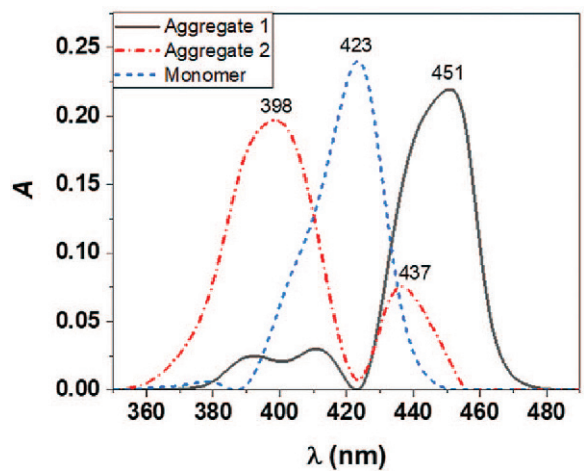

Figure 10. Spectral components of ThCy identified by MCR analysis.

https://doi.org/10.1346/CCMN.2018.064090 Published online by Cambridge University Press

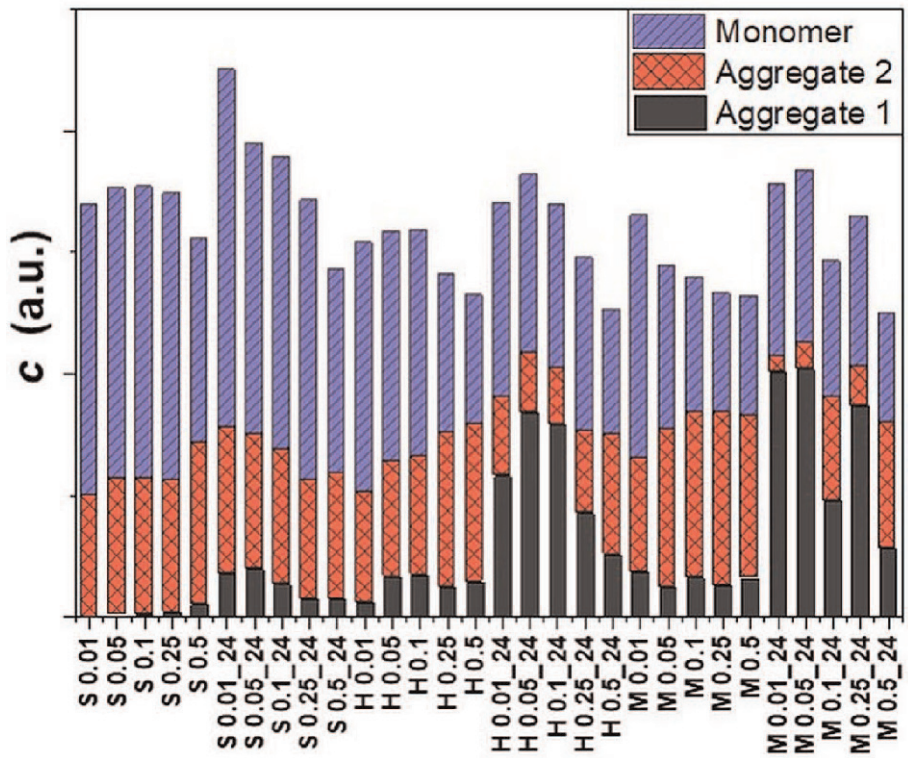

Figure 11. Concentrations of the spectral components of ThCy/Smectite, as determined by MCR analysis. Markings on the horizontal axis indicate the samples. The abbreviations used indicate Clay/Loading/Time. The abbreviations of the clay-mineral names are as follows: S (saponite), H (hectorite), and M (montmorillonite).

time. This behavior is similar to the aggregation of methylene blue in Mnt dispersions (Bujdák *et al.*, 2001). On the other hand, this behavior is opposite to that of rhodamine dyes in smectite dispersions (Lofaj and Valent, 2013; Baranyaiová and Bujdák, 2015).

The fluorescence behavior of the colloids containing ThCy depended most heavily on the type of smectite (Figure 12). The highest relative emission was observed for the ThCy/Sap colloid with the lowest loading (0.01 mmol/g). Increasing the concentration of the dye on the Sap surface led to a significant decline in emission. Clearly, the presence of molecular aggregates was largely responsible for this phenomenon. Hec and Mnt colloids exhibited very low fluorescence and the effect of the ThCy loading was much lower than the influence of the surface properties of smectites. An interesting feature was the emission of J-aggregates, with relatively sharp emission bands and a low Stokes shift (based on the comparison between absorption and emission spectra). Interestingly, a significant increase was noted in fluorescence intensity on formation of J-aggregates in the ThCy/Mnt colloids over time (Figure 12c, dashed lines).

CONCLUSIONS

Chemometric methods provided excellent tools for detailed analysis of the interactions between organic dyes and smectites. The dye OxCy, which exists as a monomer with two conformational isomers, formed two structurally similar oblique aggregates on the smectite surface. These two types of aggregates were not apparent from the spectra, but could be distinguished by chemomentric analysis. The oblique aggregates were probably associated with the assemblies formed from the two different conformational isomers of this dye. Interestingly, these aggregates exhibited a similar splitting of the excitation energy, observable by the energy difference between H- and J-bands, which was around 2470 and 2080 cm^{-1}, respectively. The dye ThCy exhibited a significantly greater tendency to form molecular aggregates. With aging of the hybrid dispersions, the emergence of a new oblique aggregate with dominant J-band was observed while the amount of oblique aggregate with dominant H-band declined. These changes had significant effects on the shape and intensity of the fluorescence bands of the dye.

A previous study discussed the role of Sap particles in the enhanced emission of ThCy dye (Boháč *et al.*, 2016). The adsorption of dye molecules prevented rotational movement of heterocyclic centers around the polymethine chain and thus reduced non-radiational relaxation of the molecules. The same behavior was observed in the present study, with dye concentration at the surface affecting the photophysical activity of both dyes. The presence of Hec

https://doi.org/10.1346/CCMN.2018.064090 Published online by Cambridge University Press

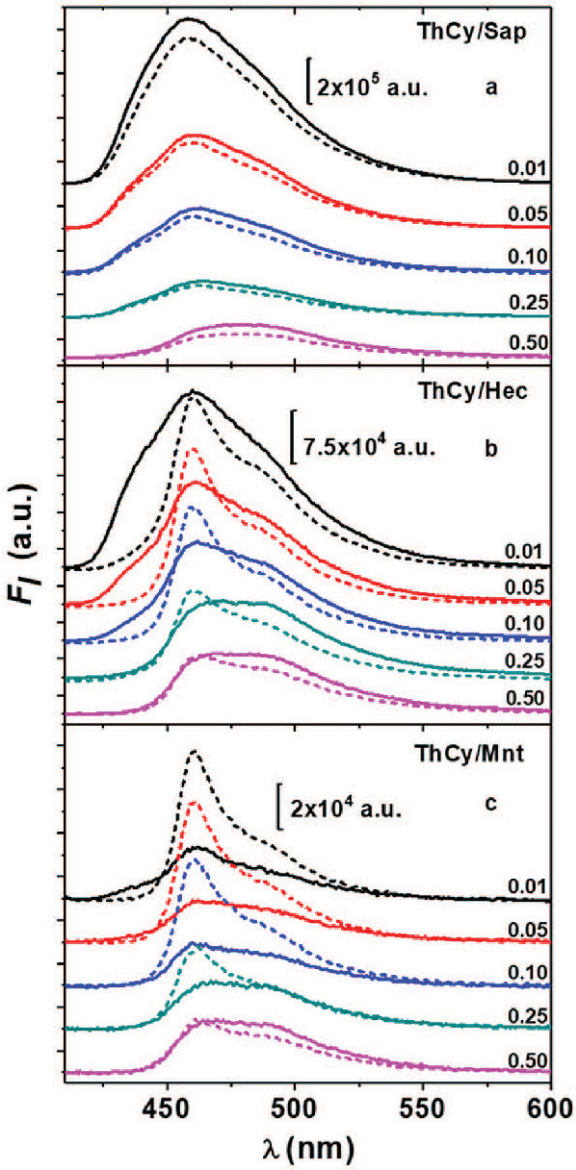

Figure 12. Emission spectra of ThCy in smectite colloidal dispersions. The solid lines represent absorption spectra recorded immediately (~1 min) after mixing the dye solution and smectite colloidal dispersion, and dashed lines represent spectra recorded 24 h after mixing.

particles caused a similar but less intense increase in emission. The role of fluorescence quenchers in reducing overall emission yield was most significant for the systems with montmorillonite. In conclusion, the surface properties of smectite particles can have the same, or an even more significant, effect on the behavior of cyanine dyes than their average concentration on the surface of the particles. The photophysical properties of cyanine dyes in smectite dispersions ultimately depend, therefore, on which of various effects – dye aggregation, dispersion stability, or the aforementioned enhancement of emission – is dominant.

The present study has produced new data on and insight into the behavior of hybrid systems composed of layered silicates and cyanine dyes. The photophysical properties of cyanine dyes can be changed completely by interaction with smectite particles, and their photoactivity can be improved by this interaction. Selection of suitable smectite and rather low dye/smectite loading seem to be important for maintaining high photoactivity of the resulting hybrid system. Another aspect is that cyanine dyes can serve as probes for determining the surface properties of clay minerals. Either absorption spectra, or the more sensitive changes in fluorescence, can be used for the characterization of clay minerals.

ACKNOWLEDGMENTS

The present study was supported by the Slovak Research and Development Agency under contract No. APVV-15-0347. Support from the VEGA grant agency (grants 1/0278/16 and 2/0156/17) is also acknowledged with gratitude.

REFERENCES

Anedda, A., Carbonaro, C.M., Clemente, F., Corpino, R., Grandi, S., Magistris, A., and Mustarelli, P.C. (2005) Rhodamine 6G-SiO_2 hybrids: A photoluminescence study. *Journal of Non-Crystalline Solids*, **351**, 1850–1854.

Baranyaiová, T. and Bujdák, J. (2015) Reaction kinetics of molecular aggregation of rhodamine 123 in colloids with synthetic saponite nanoparticles. *Applied Clay Science*, **134**, 1–7.

Behera, G.B., Behera, P.K., and Mishra, B.K. (2007) Cyanine dyes: Self aggregation and behaviour in surfactants: A review. *Journal of Surface Science and Technology*, **23**, 1–31.

Bergmann, K. and O'Konski, C. (1963) Spectroscopic study of methylene blue monomer, dimer and complexes with montmorillonite. *Journal of Physal Chemistry*, **67**, 2169–2177.

Boháč, P., Czímerová, A., and Bujdák, J. (2016) Enhanced luminescence of 3,3'-diethyl-2,2'-thiacyanine cations adsorbed on saponite particles. *Applied Clay Science*, **127–128**, 64–69.

Bujdák, J. (2006) Effect of the layer charge of clay minerals on optical properties of organic dyes. A review. *Applied Clay Science*, **34**, 58–73.

Bujdák, J. and Komadel, P. (1997) Interaction of methylene blue with reduced charge montmorillonie. *Journal of Physical Chemistry, B*, **101**, 9065–9068.

Bujdák, J., Janek, M., Madejová, J., and Komadel, P. (1998) Influence of the layer charge density of smectites on the interaction with methylene blue. *Journal of the Chemical Society, Faraday Transactions*, **94**, 3487–3492.

Bujdák, J., Janek, M., Madejová, J., and Komadel, P. (2001) Methylene blue interactions with reduced-charge smectites. *Clays and Clay Minerals*, **49**, 244–254.

Bujdák, J., Iyi, N., Hrobáriková, J., and Fujita, T. (2002a) Aggregation and decomposition of a pseudoisocyanine dye in dispersions of layered silicates. *Journal of Colloid and Interface Science*, **247**, 494–503.

Bujdák, J., Iyi, N., and Fujita, T. (2002b) The aggregation of methylene blue in montmorillonite dispersions. *Clay Minerals*, **37**, 121–133.

Bujdák, J., Iyi, N., and Fujita, T. (2003) Control of optical properties of adsorbed cyanine dyes via negative charge

https://doi.org/10.1346/CCMN.2018.064090 Published online by Cambridge University Press

distribution on layered silicates. *Solid State Phenomena*, **90-91**, 90–91.

Carbonaro, C.M. (2011) Chemistry tuning the formation of aggregates in silica – Rhodamine 6G hybrids by thermal treatment. *Journal of Photochemistry & Photobiology, A: Chemistry*, **222**, 56–63.

Chibisov, A.K., Slavnova, T.D., and Görner, H. (2006) Kinetics of J-aggregation of a thiacarbocyanine dye in aqueous solution: Novel aggregate mediated by alcohols and metal ions. *Chemical Physics Letters*, **424**, 307–311.

Czímerová, A., Bujdák, J., and Dohrmann, R. (2006) Traditional and novel methods for estimating the layer charge of smectites. *Applied Clay Science*, **34**, 2–13.

Eisfeld, A. and Briggs, J.S. (2006) The J- and H-bands of organic dye aggregates. *Chemical Physics*, **324**, 376–384.

Gemeay, A.H., El-Sherbiny, A.S., and Zaki, A.B. (2002) Adsorption and kinetic studies of the intercalation of some organic compounds onto Na^+-montmorillonite. *Journal of Colloid and Interface Science*, **245**, 116–125.

Hranisavljevic, J. and Wiederrecht, G.P. (2012) Kinetics of J-aggregate formation on the surface of Au nanoparticle colloids. *Journal of Physical Chemistry, C*, **116**, 4655–4661.

Kaufhold, S. (2006) Comparison of methods for the determination of the layer charge density (LCD) of montmorillonites. *Applied Clay Science*, **34**, 14–21.

Kometani, N., Nakajima, H., Asami, K., Yonezawa, Y., Scheblykin, I.G., and Vitukhnovsky, A.G. (2000) Luminescence properties of the J-aggregate of cyanine dyes in multilayer assemblies. *Journal of Luminescence*, **87**, 770–772.

Lofaj, M. and Valent, I. (2013) Mechanism of rhodamine 6G molecular aggregation in montmorillonite colloid. *Central European Journal of Chemistry*, **11**, 1606-1619

López Arbeloa, F., Aguirresacona, I.U., and López Arbeloa, I. (1989) Influence of the molecular structure and the nature of the solvent on the absorption and fluorescence characteristics of rhodamines. *Chemical Physics*, **130**, 371–378.

López Arbeloa, F., Martínez Martínez, V., Arbeloa, T., and López Arbeloa, I. (2007) Photoresponse and anisotropy of rhodamine dye intercalated in ordered clay layered films. *Journal of Photochemistry and Photobiology C: Photochemistry Reviews*, **8**, 85–108.

Matejdes, M., Himeno, D., Suzuki, Y., and Kawamata, J. (2017a) Controlled formation of pseudoisocyanine J-aggregates in the interlayer space of synthetic saponite. *Applied Clay Science*, **140**, 119–123.

Matejdes, M., Himeno, D., Suzuki, Y., and Kawamata, J. (2017b) The effect of the negative charge density on switchable properties of pseudoisocyanine dye. *Applied Clay Science*, **144**, 54–59.

Miyamoto, N., Kawai, R., Kuroda, K., and Ogawa, M. (2000) Adsorption and aggregation of a cationic cyanine dye on layered clay minerals. *Applied Clay Science*, **16**, 161–170.

Nakato, T., Inoue, S., Hiraragi, Y., Sugawara, J., Mouri, E., and Aritani, H. (2014) Decomposition of a cyanine dye in binary nanosheet colloids of photocatalytically active niobate and inert clay. *Journal of Materials Science*, **49**, 915–922.

Ogawa, M. (1998) Organized molecular assemblies on the surfaces of inorganic solids-photofunctional inorganic-organic supramolecular systems. *Annual Reports on the Progess of Chemistry*, **94**, 209–257.

Ogawa, M. and Kuroda, K. (1995) Photofunctions of intercalation compounds. *Chemical Reviews*, **95**, 399–438.

Ogawa, M., Kawai, R., and Kuroda, K. (1996) Adsorption and aggregation of a cationic cyanine dye on smectites. *Journal of Physal Chemistry*, **100**, 16218–16221.

Ono, S.S., Yao, H., O.M., Kawabata, R., Kitamura, N., and Yamamoto, S. (1999) Anisotropic growth of J aggregates of pseudoisocyanine dye at a mica/solution interface revealed by AFM and polarization absorption measurements. *Journal of Physical Chemistry B*, **103**, 6909–6912.

Pasternack, R.F., Fleming, C., Herring, S., Collings, P.J., dePaula, J., DeCastro, G., and Gibbs, E.J. (2000) Aggregation kinetics of extended porphyrin and cyanine dye assemblies. *Biophysical journal*, **79**, 550–60.

Pomogailo, A.D. (2005) Hybrid intercalative nanocomposites. *Inorganic Materials*, **41**, 47–74.

Roden, J., Eisfeld, A., and Briggs, J.S. (2008) The J- and H-bands of dye aggregate spectra: Analysis of the coherent exciton scattering (CES) approximation. *Chemical Physics*, **352**, 258–266.

Sato, N., Fujimura, T., Shimada, T., Tani, T., and Takagi, S. (2015) J-aggregate formation behavior of a cationic cyanine dye on inorganic layered material. *Tetrahedron Letters*, **56**, 2902–2905.

Shapiro, B.I. (2007) Aggregates of cyanine dyes: Photographic problems. *Russian Chemical Reviews*, **63**, 231–255.

Shapiro, B.I., Manulik, E.V., and Prokhorov, V.V. (2016) Multilayer J-aggregates of cyanine dyes. *Nanotechnologies in Russia*, **11**, 265–272.

Schoonheydt, R. and Johnston, C.T. (2013) *Surface and Interface Chemistry of Clay Minerals*. Pp. 87–113 in: *Handbook of Clay Science* (F. Bergaya and G. Lagaly, editors), 2nd edition. Elsevier Ltd., Amsterdam.

Schulz-Ekloff, G., Wöhrle, D., van Duffel, B., and Schoonheydt, R.A. (2002) Chromophores in porous silicas and minerals: Preparation and optical properties. *Microporous and Mesoporous Materials*, **51**, 91–138.

Smirnov, M.S., Ovchinnikov, O.V., Dedikova, A.O., Shapiro, B.I., and Vitukhnovsky, A.G. (2016) Luminescence properties of hybrid associates of colloidal CdS quantum dots with J-aggregates of thiatrimethine cyanine dye. *Journal of Luminescence*, **176**, 77–85.

Tani, K., Ito, C., Hanawa, Y., Uchida, M., Otaguro, K., Horiuchi, H., and Hiratsuka, H. (2008) Photophysical property and photostability of J-aggregate thin films of thiacyanine dyes prepared by the spin-coating method. *Journal of Physical Chemistry, B*, **112**, 836–844.

Tillmann, W. and Samha, H. (2004) J-aggregates of cyanine dyes in aqueous solution of polymers: A quantitative study. *American Journal of Undergraduate Research*, **3**, 1–6.

Valandro, S.R., Poli, A.L., Correia, F.A., Lombardo, P.C., Schmitt, C.C., and Postal, C. (2017) Photophysical behavior of isocyanine/clay hybrids in the solid state. *Langmuir*, **33**, 891–899.

Würthner, F., Kaiser, T.E., and Saha-Möller, C.R. (2011) J-aggregates: From serendipitous discovery to supramolecular engineering of functional dye materials. *Angewandte Chemie – International Edition*, **50**, 3376–3410.

Yonezawa, Y., Yamaguchi, A., and Kometani, N. (2005) Exciton delocalization of the J-aggregate of oxacyanine dye and thiacyanine dye in LB films. *Physica Status Solidi, B*, **242**, 803–806.

Zhu, Z. (1995) Thirty-five years of studies on the chemistry of polymethine cyanine dyes. *Dyes and Pigments*, **27**, 77–111.

(*Received 15 October 2017; revised 19 March 2018; Ms. 1224; AE: J.W. Stucki*)